Relaxation processes due to the electrode-electrolyte interface in ionic solutions

Hugo Sanabria* and John H. Miller, Jr.†
Department of Physics and the Texas Center for Superconductivity at the University of Houston, University of Houston, Houston, Texas, 77204, USA

(Received 3 March 2006; revised manuscript received 27 July 2006; published 20 November 2006)

One of the major challenges in electrochemistry is to properly account for polarization of the electrical double layer that forms at an electrode-electrolyte interface, especially when interpreting the impedance spectra of biological molecules, electrolytes, or live cell suspensions. This double layer, which affects the measured impedance, is also known as the electrode polarization effect. Various methods of correcting for its effects on impedance data have been reported, including varying the spacing between electrodes, four-electrode techniques, and electrodeless methods. Here we discuss the use of a constant phase element in a recently proposed circuit model, which can be thought of as a measure of the fractal nature of the interface. We also report on the conductivity spectra of several saline solutions over the frequency range 1 Hz–1 MHz, in which we observe Debye-like relaxation behavior that changes with ion concentration and type. Good agreement is obtained with an alternative model that treats the cations and anions as overdamped oscillators in harmonic restoring potentials.

DOI: 10.1103/PhysRevE.74.051505 PACS number(s): 82.45.Fk, 73.30.+y, 82.45.Gj, 77.84.Nh

I. INTRODUCTION

Dielectric studies of live cells and biological molecules in suspension have been carried out for over 75 years [1,2], and have revealed information about cellular membrane potentials, macromolecular charges, dipole moments, and field-induced conformational changes. However, both time- and frequency-domain impedance spectroscopy measurements suffer from the electrode polarization (EP) effect [3,4], in which an electrical double layer forms at the electrode-electrolyte interface and becomes polarized. Numerous studies have led to a number of approaches to correct for this phenomenon. We can group these into two main categories.

The first category uses experimental techniques, such as electromagnetic induction [5,6] and a four-probe method [7–11], where two electrodes drive the system while the other two record the signal to reduce current flow through the voltage electrodes. However, the four-electrode method does not eliminate the polarization effect, which is always present wherever there is an interface between surface charges in a metal and an electrolyte. Another method within this group is to vary the spacing between electrodes [2,12–14], which works best for separation distances that are large compared with the electrode diameters. Unfortunately, this is not feasible when the amount of liquid is restricted, especially when working with biomolecules at high concentration [15].

The second category includes models that incorporate the impedance produced by the polarization effect into the total impedance. Such models include the use of a capacitive layer between the electrode and the bulk. One example is the use of a constant phase element (CPE) impedance [16,17], which will be discussed in this paper, and a model presented here, in which we represent the motion of ions close to the interface as overdamped oscillators in a restoring harmonic potential.

The motivation for this work is to explore the proposed methods to account for the EP effect based on the understanding of the basic mechanisms underlying the double layer. One method presented here models the double layer as a polarization impedance, which adds another linear element to the electric circuit model as a result of a phenomenological description of the observed data. The EP effect takes place at the electrode-electrolyte interface, where chemical reactions sometimes occur. It is here that the diffusion of ions close to the surface charges of the electrode plays an important role, primarily at low frequencies, making it very difficult to interpret measurements of highly conductive samples, such as aqueous biological solutions [4,15,18]. One proposed mechanism for interpreting the impedance resulting from the EP effect is to model surface roughness by considering a random walk of charged ions in proximity to the electrode surface. This theoretical approach yields a CPE impedance with power-law behavior, and has been related to the fractal nature of the electrode roughness [4,19,20]. However, the surface topology and the power law do not seem to correlate as previously reported by Bates *et al.* [21]. Several years later, Larsen *et al.* [22] showed that, by electrochemical deposition onto copper electrodes in an aqueous solution containing 0.01 M $CuSO_4$, they could experimentally create fractal electrodes that support the predicted behavior using Halsey-Leibig theory. One should note that designing an experiment to prove the effect of the fractal nature of the surface topology is a complicated task, because of the limitations on controlling fractal surfaces at very small dimensions. Although both theory and experiments have shown that the electrodes play a fundamental role in the impedance spectrum at lower frequencies, additional experiments suggest that different electrolytes, polar and nonpolar solutions, are important to the behavior of the impedance spectrum at low frequencies.

The double-layer impedance has also been modeled as a parallel resistor-capacitor network in series with a second

*Electronic address: Hugo.Sanabria@uth.tmc.edu
†Electronic address: jhmiller@mail.uh.edu

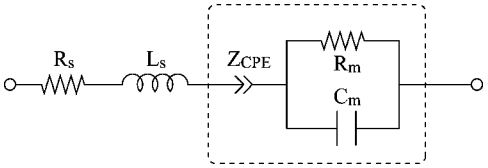

FIG. 1. Equivalent circuit for a conductive electrolyte where the double layers are represented as a constant phase element impedance Z_{CPE}.

resistor, as described by the Randles equivalent circuit [23]. This circuit model has been used to describe the ac response with charge transfer and diffusion of the electroactive species. A simplified version of this is to consider a single capacitor in series with a well-define resistance [9] to account for the EP. The capacitive energies of charged particles in or near the double layer are formally similar to those of particles, whose motions are highly damped in a viscous environment, in a harmonic potential (overdamped oscillator model), as we will discuss in greater detail later in this paper.

In this paper, we present a comparison of the above two approaches to account for the polarization effect. In Sec. II, we model the double layer as a CPE element, the parameters of which are extracted from experimental data. Section III discusses the experimental measurements, while Sec. IV presents a theoretical model of the behavior of the ions close to the interface, which gives qualitative agreement with the data. We present our assumptions in Sec. V as well as our justification for the use of the overdamped oscillator, and finally we summarize in Sec. VI.

II. ELECTRIC CIRCUIT MODEL WITH CPE IMPEDANCE

When modeling the polarization impedance, we have to consider that the electrical double layer takes place at the two-electrode interfaces. The model in Fig. 1 assumes the polarization impedance to be the same at both electrodes, which are then combined into a single constant phase element (CPE) with an impedance described by

$$Z_{\mathrm{CPE}} = \frac{1}{T(i\omega)^p}. \tag{1}$$

The cable impedance, considered as a series combination of a resistor R_s and inductor L_s, is obtained by shorting the electrodes and measuring the total impedance. The impedance of the conductive electrolyte being measured is modeled as a capacitor C_m in parallel with a resistor $R_m = d/\sigma' A$, where d, A, and σ' are the electrode spacing, the area of each electrode, and conductivity of the medium,

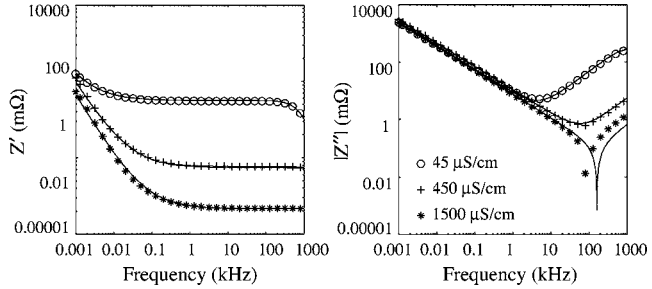

FIG. 2. Real (Z') and imaginary (Z'') part of the measured total impedances of three calibration solutions with known conductivities. The solid lines are theoretical plots using the circuit model shown in Fig. 1 and described by Eq. (2). The fitting parameters of the correspondent solid lines are shown in Table I. $|Z''|$ is plotted as the absolute value for logarithmic display, but $|Z''|$ actually becomes negative for frequencies above $\sim 10^5$ Hz for the highest conductivity solution. ○, 45 μS/cm; +, 450 μS/cm; ∗, 1500 μS/cm.

respectively. The total complex impedance (Z_T^*) or admittance (Y_T^*) of the network is thus given by

$$Z_T^* = \frac{1}{Y_T^*} = R_s + i\omega L_s + Z_{\mathrm{CPE}} + \frac{1}{1/R_m + i\omega C_m}, \tag{2}$$

where the capacitance takes the usual form, $C_m = \epsilon' \epsilon_0 A/d$, and ϵ' is the real part of the dielectric constant of the medium.

As a control experiment, we tested this model with three different calibration standard solutions purchased from Omega Inc. with known conductivities (45, 450, and 1500 μS/cm). The data in symbols and the theoretical fits with solid lines are shown in Fig. 2. The model presented shows good agreement with the expected conductivity values given by the standard solutions (see Table I). The agreement is better as the conductivity increases, since the capacitive effect is screened by the conductivity. Also, for this particular set of controls, p is very stable at a value of ~ 0.82. This will become relevant later on in the discussion.

III. EXPERIMENTAL RESULTS

We prepared several saline solutions of KCl, $MgCl_2$, $CaCl_2$, and NaCl at concentrations ranging from 1 μM to 500 mM. We measured the total impedance with a Solartron 1260 impedance analyzer connected to a liquid holder with stainless-steel electrodes with a cell constant d/A, where $d=1$ mm is the separation distance between the electrodes and $A=\pi r^2$ is the cross-sectional area of the elec-

TABLE I. Fitting parameters used in the model described by Eq. (2).

Sample	T (Ss^p)	p	R_m (Ω)	C_m (nF)	σ (μS/cm)
45 μS/cm	8.7×10^{-5}	0.82	560.3	0.24	56.8
450 μS/cm	7.0×10^{-5}	0.82	74.0	0.21	430.6
1500 μS/cm	8.6×10^{-5}	0.83	21.2	0.20[a]	1506.0

[a]This value does not change the fitting, since the conductivity is too high, and mostly all the current will flow through the conductance.

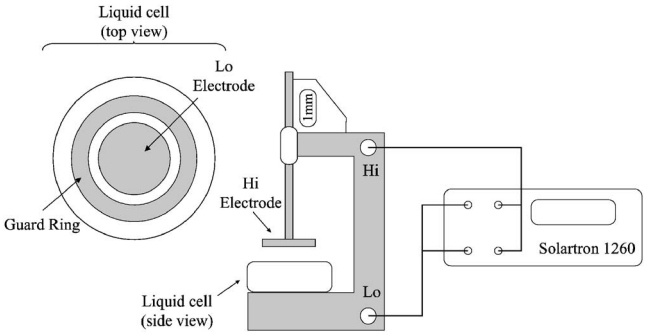

FIG. 3. Experimental setup using an impedance analyzer (Solartron 1260) to sweep the frequency from 1 Hz to 1 MHz connected to a liquid sample holder, which has a guard ring to reduce stray field effects.

trodes, where $r=1$ cm. The bottom electrode has a guard ring that reduces stray capacitance produced by the finite size of the electrodes. The frequency range tested was from 1 Hz to 1 MHz (see Fig. 3), and the data acquisition was performed using SMART®, a Solartron analytical software.

The results in Figs. 4 and 5 show the real and imaginary part of the conductivity spectrum ($\sigma^*=1/Y_T^*$), respectively, for the different ionic solutions in units of μS/cm. It is clear from these plots that as the concentration of the ions is increased, independently of the type of ions, there is a relaxation process that takes place at frequencies <kHz. This relaxation depends on the ion concentration, as it shows the same behavior for all the solutions. We analyzed the behavior of concentration below 100 mM because the data show minimum noise. At these concentrations we have conductivities on the order of mS/cm, as in the case of one of the samples used for calibration; see Table I.

To analyze the data, we performed a nonlinear complex fitting using a commercial program for circuit analysis (ZVIEW®). The circuit model presented in Fig. 1 including a CPE element for the polarization impedance was used in the analysis. In this case, the parameters obtained from the fitting routine are shown in Figs. 6 and 7 with respect to the different concentrations and ion type.

The parameter $0<p<1$ has been related to the fractal dimension of the electrode surface [3]. In our experiments, p differs between solutions, and the parameter T varies significantly as a function of the electrolyte used. This is an indication that the relaxation will depend not only on the physical properties of the electrodes, but also is a function of the electrolyte that is in contact with the electrode. However, the range of values is consistent with previously reported values of $p=0.78$ [3] using stainless-steel electrodes. Since such electrodes were not the same as the ones used in this study, we can assign such differences to changes on the surface roughness, remembering that $p=1$ would represent a perfectly flat electrode, as in the case of a capacitor. T, with units of Ss^p (S corresponds to Siemens, s to seconds, and p to the power-law exponent; remember that 1 Farad is 1 Ss), could be interpreted as a capacitance, but it is evident that their units do not match. If the CPE element were to have a $p=1$, then the CPE will behave exactly as a capacitor. In this case, T would depend on the dielectric properties of the solution close to the interface of the double layer. For example, using $T=8\times10^{-5}$, and if one were to take the dielectric constant for water $\epsilon'\sim80$ and the cross-sectional area A used in this experiment, one could obtain a thickness $d=2.7$ nm. Clearly this distance could be related to the double layer because it is consistent with the expected Debye length of a few nm.

The fitting parameters also gave us the conductivity for each of the solutions (Fig. 8), and, as mentioned in the Introduction, the fitting for commercial standard calibration solutions gave good agreement with the reported value at higher conductivities. This approach allows a calibration for high conductivity samples where one can extract with good confidence the real value of the conductivity and define the polarization impedance and subtract it in further experiments.

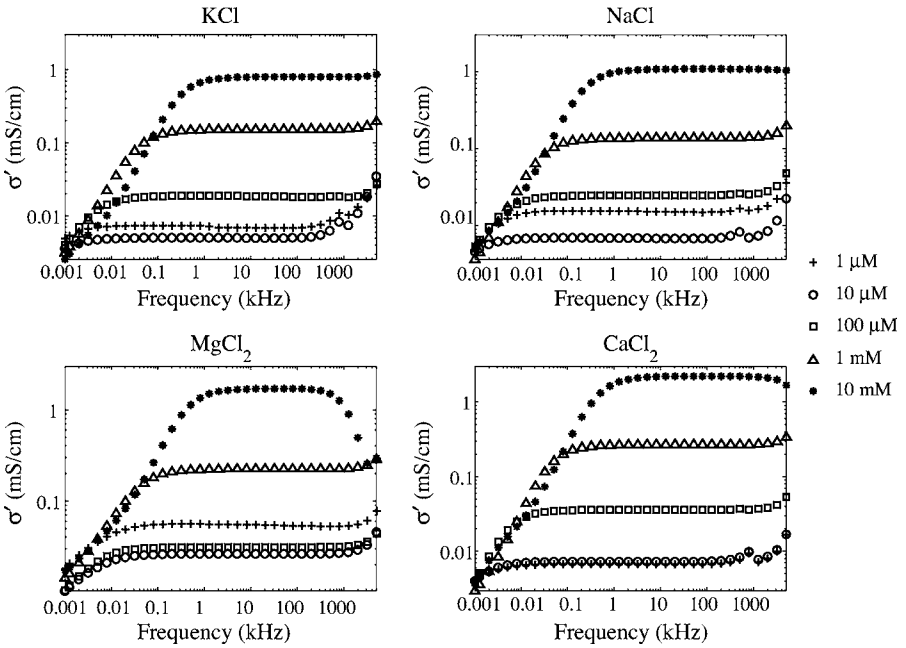

FIG. 4. Real part of admittance (σ') vs frequency for different concentration and several saline solutions. +, 1 μM; ○, 10 μM; □, 100 μM; △, 1 mM; and ∗, 10 mM.

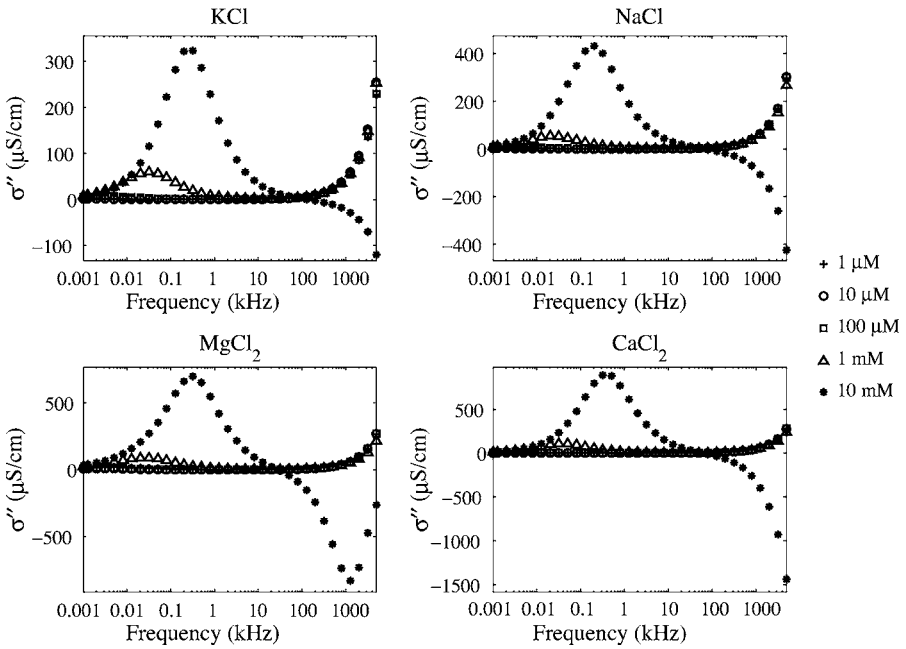

FIG. 5. Imaginary part of admittance (σ'') vs frequency for different concentration and several saline solutions. +, 1 μM; ○, 10 μM; □, 100 μM; △, 1 mM; and ∗, 10 mM.

With this treatment, is very difficult of give an interpretation of the polarization impedance, or the electrode polarization effect. However, many authors [3,4,20] use the power-law behavior of the polarization impedance (CPE) and relate it with the fractal properties of the electrode electrolyte interface. Theoretically, this phenomenon was believed to occur at higher frequencies, because at low frequencies the mobility of the ions is predominantly governed by diffusion.

In addition, let us recall that by performing the fits using the model described in this section, the capacitance, and hence the dielectric permittivity as well as the conductivity that are obtained from the fitting routine, will not vary with respect to the frequency. Thus this process will work only for characterizing the electrodes and finding the polarization impedance, but the frequency dependence of the electrolyte is lost.

Similar models include a capacitive element to describe the double layer. One particular example is the Randles equivalent circuit. This circuit is valid in an electrochemical system with either a charge transfer or diffusion-limited kinetics [24]. In the parallel network, the resistive element represents the charge transfer and the capacitance represents the double layer. Regardless of which electrical network is used to model the interface between the electrode and electrolytes, the model requires a capacitive-like element to describe the EP coupled to another linear element. When a capacitance is used to model the double layer, the network acts as a high pass filter; this is shown experimentally and with the current models in the literature. However, sometimes we are interested in the low-frequency impedance response of different biological dilutions to extract physical properties of various molecules. This would eventually become possible if the model that describes the EP incorporates physical mechanisms that involve the solution and not only the surface topology of the electrodes. For this reason, in the following section we present an overdamped harmonic-oscillator model that allows us to relate the restoring force with the charge and dielectric properties of the medium.

IV. HARMONIC RESTORING POTENTIAL MODEL

The double-layer effect, as shown from the data, produces a relaxation at frequencies that depend on the concentration of ions in solution. Having in mind the behavior observed at higher concentration, such as the case of 10 mM, it is clear

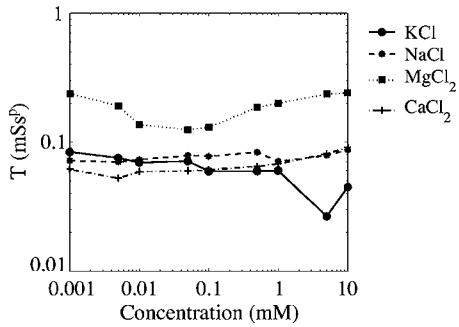

FIG. 6. T component of the CPE for the different ionic solutions.

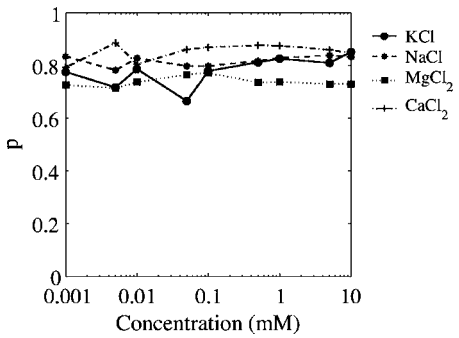

FIG. 7. Exponent p on the CPE, sometimes called fractal dimension for the different ionic solutions.

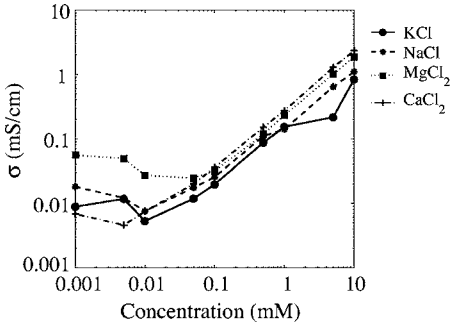

FIG. 8. Conductivity vs concentration for various saline solutions.

from Fig. 5 that the imaginary part of the conductivity goes to negative values showing a second bell-shaped curve at around 10^6 Hz. This type of behavior is found in overdamped oscillators. Thus, one can think of the motion of each ion j as being described by a heavily damped harmonic oscillator with a natural resonant frequency ω_0, a charge q_j, and mass m_j. In the presence of an applied electric field $E(t)$, the equation of motion is written as

$$\frac{d^2x_j}{dt^2} + \gamma_j \frac{dx_j}{dt} + \omega_{0_j}^2 x = \frac{q_j}{m_j} E. \tag{3}$$

In other words, the ions are oscillating near the interface with the electrode, and the motion is overdamped with a dissipating force as a function of different mechanism, such as Stoke's drag force, which is a function of the fluid's viscosity, and the dimension of ions. Other collisional interactions will also dissipate energy in a similar fashion, and we attribute γ to include all of the possible factors that damped the oscillator.

To solve the equation of motion, let us consider the applied electric field has the form $E(t)=E_0 \exp(i\omega t)$, while the position of the ions is written as $x_j(t)=x_{0_j} \exp(i\omega t)$. The frequency response is then expressed as

$$(\omega_{0_j}^2 - \omega_j^2 + i\gamma_j\omega)x_{0_j} = \frac{q_j}{m_j} E_0. \tag{4}$$

We then write the current density as

$$J_j = \frac{N_j q_j}{V} \frac{dx_j}{dt}, \tag{5}$$

where N_j is the number of ions j in the volume V. With $J_j=J_{0_j} \exp(i\omega t)$, we obtain

$$J_{0_j} = \frac{i\omega\sigma_{m_j}}{\omega_{0_j}^2 - \omega^2 + i\gamma_j\omega} E_0, \tag{6}$$

where $\sigma_{m_j}=N_j q_j^2/mV$, and the complex conductivity is defined as

$$\sigma_j^*(\omega) = J_{0_j}/E_{0_j}, \tag{7}$$

$$= \sigma_j' + i\sigma_j'', \tag{8}$$

$$= \frac{d}{A} Y_T^*(\omega), \tag{9}$$

and can be separated into real and imaginary parts as follows:

$$\sigma_j'(\omega) = \frac{\sigma_{m_j}\gamma_j\omega^2}{(\omega_{0_j}^2 - \omega^2)^2 + \gamma_j^2\omega^2}, \tag{10}$$

$$\sigma_j''(\omega) = \frac{\sigma_{m_j}\omega(\omega_{0_j}^2 - \omega^2)}{(\omega_{0_j}^2 - \omega^2)^2 + \gamma_j^2\omega^2}. \tag{11}$$

The fitted data are shown in Fig. 9, and the fitted parameters are shown in Table II. They were obtained using

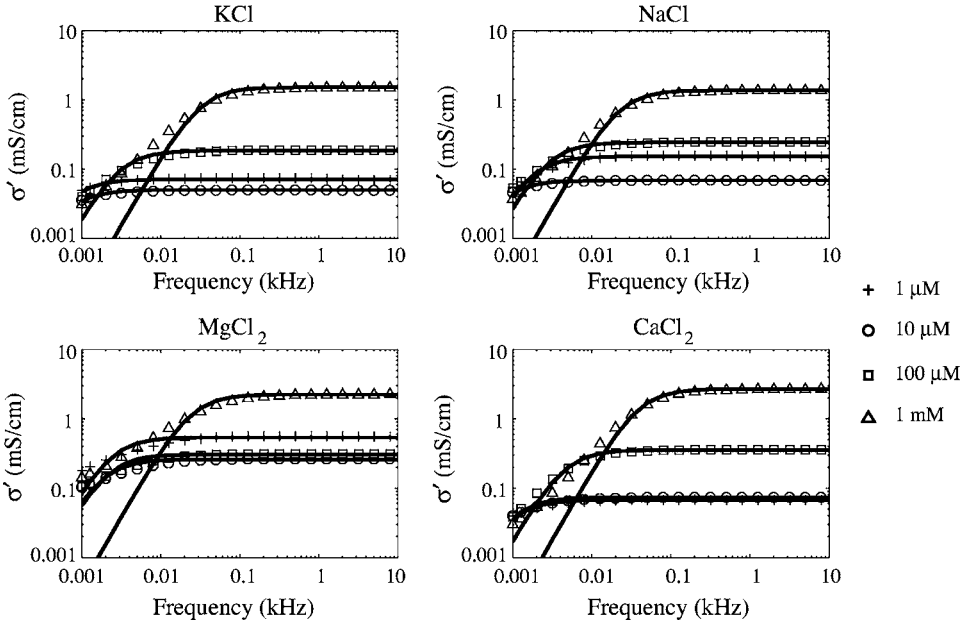

FIG. 9. Real part of the conductivity spectrum for different saline solutions at three different concentrations. The data were fitted using the harmonic-oscillator model with $i=1$. +, 1 μM; ○, 10 μM; □, 100 μM; and △, 1 mM.

TABLE II. Fitting parameters of Eq. (10) with a single component ($i=1$).

Solution	Concentration (μM)	σ_m (μS/cm)	γ (Hz)	ω_0 (Hz)
KCl	10^1	4.91×10^6	9.82×10^5	814.58
	10^2	1.45×10^7	7.89×10^5	1526.9
	10^3	3.16×10^7	2.07×10^5	2550.6
NaCl	10^1	6.18×10^6	8.97×10^5	819.47
	10^2	1.51×10^7	6.21×10^5	1327.6
	10^3	2.95×10^7	2.15×10^5	2189.4
$MgCl_2$	10^1	1.57×10^7	6.03×10^5	1040.9
	10^2	1.72×10^7	5.62×10^5	1090.2
	10^3	4.56×10^7	2.03×10^5	2215.5
$CaCl_2$	10^1	6.37×10^6	8.69×10^5	940.95
	10^2	1.83×10^7	5.17×10^5	1519
	10^3	5.42×10^7	2.02×10^5	2802.8

a nonlinear square fitting from MATLAB (Mathworks) *lsqcurvefit*. In this case, a single component ($i=1$) was considered.

The model presented above is an alternative model to explain impedance data at low frequencies where the electrode polarization effect or diffusive layer plays a major role. Using this set of equations, one obtains a qualitative agreement with these data. Also, one could see that as n (number of ions) increases, σ_{m_i} also increases as expected, and that ω_0 increases as the concentration increases. This is due to changes produced by the electric field surrounding the ions, which will change the local properties of the environment. In addition, it is clear that the comparison between theory and experiment is very good at low concentrations, where the dynamics is best described with the contribution of one ion i; however, for higher concentrations the conductivity is best described by

TABLE III. Parameters used to fit Fig. 10 with Eq. (10) with an additional dc component σ_{dc} using a two-component model ($i=2$) were obtained at 10 mM concentrations of KCl, NaCl, $MgCl_2$, and $CaCl_2$.

Parameter	KCl	NaCl	$MgCl_2$	$CaCl_2$
σ_{dc} (μS/cm)	1.5	4.0	13.0	3.0
σ_{m_1} (μS/cm)	2.5×10^9	3.2×10^{10}	1.7×10^{10}	1.0×10^{10}
γ_1 (Hz)	3.0×10^8	3.1×10^7	1.1×10^7	5.0×10^6
ω_{0_1} (Hz)	3.6×10^4	6.0×10^4	5.5×10^4	3.72×10^4
σ_{m_2} (μS/cm)	1.0×10^{10}	1.0×10^{10}	2.5×10^{10}	8.0×10^9
γ_2 (Hz)	1.3×10^7	5.0×10^8	5.0×10^8	3×10^8
ω_{0_2} (Hz)	5.5×10^4	5.0×10^4	5.0×10^4	4.0×10^4

$$\sigma_T^* = \sigma_{dc} + \sum_i \sigma_i^* \tag{12}$$

or a multicomponent model for each of the ions present in solution. An additional dc-conductivity σ_{dc} has been included.

In this particular case, the contribution of two relaxation processes gives a better description of the physical system because there are positive and negative ions in solution; for such a case, $i=2$. The fitting of the data for higher concentrations using this two-relaxation-process model is shown in Fig. 10, where we see a better agreement at lower frequencies, but the behavior at low frequencies may be more complicated, as shown by the discrepancy in the fittings and the data. To better fit the data at higher concentrations, a dc component (σ_{dc}) was added to Eq. (10); the fitted parameters are summarized in Table III.

From Figs. 9 and 10 we observe that a dc component is required to fit higher concentration data, which could be due to an oxide layer on the surfaces. The simple harmonic-

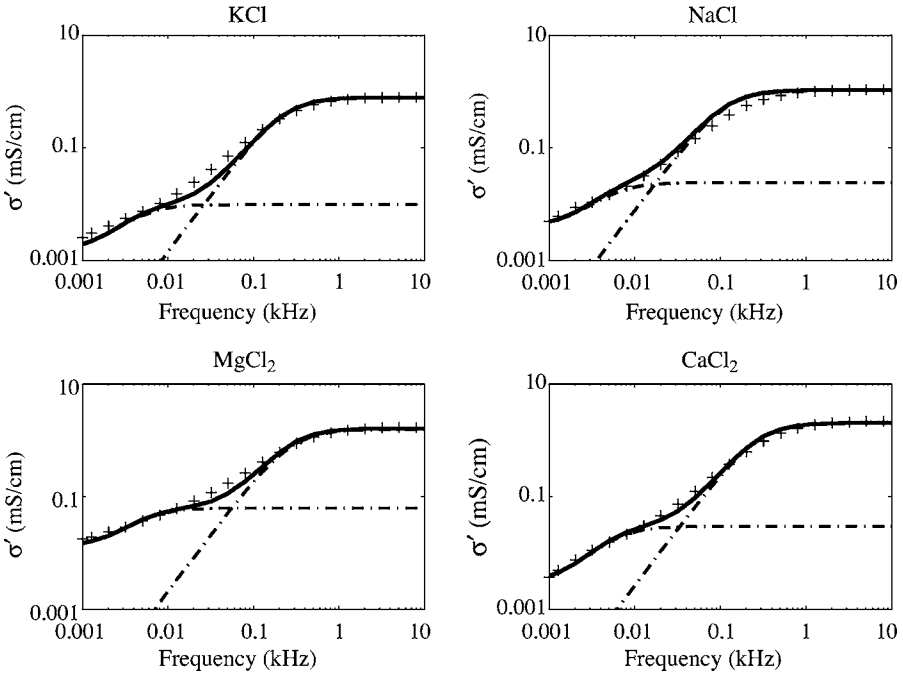

FIG. 10. Real part of the conductivity spectrum for different saline solutions at 10 mM, where the solid line represents the sum of the two contributions of the conductivity $i=2$; each contribution is shown as a dotted line.

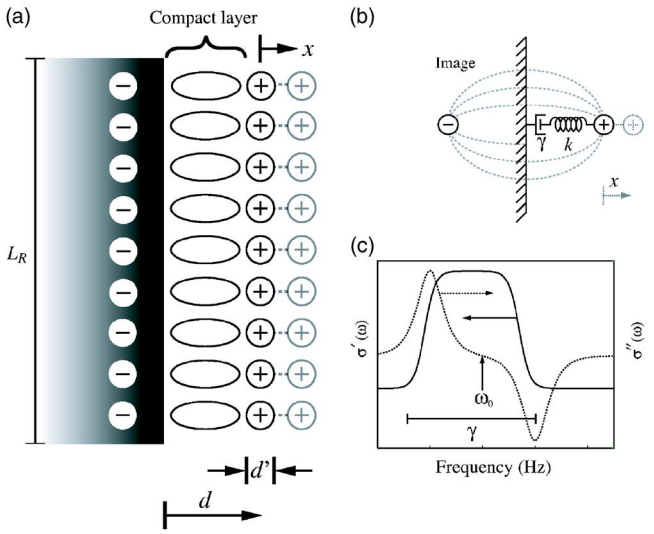

FIG. 11. (Color online) Schematic model of the overdamped harmonic oscillator as an approximation of the double layer. Panel (a) shows a sheet of charges interacting with its image. Some of the characteristic distances that are considered in our assumptions are also drawn. In panel (b), the interaction of a single charge with its image is drawn with the electric-field lines as expected from electrostatics. Also the harmonic-oscillator model is represented as a spring with a characteristic constant k and overdamped by a frictional force constant γ. Panel (c) shows an example figure of the real and imaginary contribution of the conductivity and the physical meaning of the parameters involved in the fit.

oscillator model presented here describes semiquantitatively the data over the entire spectrum, though a more detailed description is needed to account for the variations at low frequencies, where other effects, such as diffusion, might be taking place.

V. DISCUSSION

The overdamped oscillator (ODO) model qualitatively describes the data, but is a simplified picture of the EP effect. From simple electrostatics, we know that the potential is nonlinear and decays exponentially from the surface. However, when considering a small-amplitude oscillatory field, one can justify the approximations contained in the ODO model as follows. For example, consider a flat region of the electrode to be described by a characteristic length $L_R > x$, where x is the displacement distance, as shown in Fig. 11(a) for a sheet of charges in the double layer. In reality, charges are not homogeneously distributed and arranged, but this drawing is used for the sole purpose of illustrating the idea of the interaction expected at the double layer. This assumption is considered to avoid any effect from the topology of the electrode, and to keep the interaction between the charge and the electrode as simple as possible. Also, this restriction leads us to consider the motion of the ions as being close to the interface, where a restoring force is felt by the charges. Such a restoring force is due to the image charge as described by Fig. 11(b), where the interaction of a single image charge is drawn. This interaction actually takes place with the whole sheet of image charges. This model of the harmonic oscillator represents an approximation of the force exerted by the image charges under the influence of large frictional forces. The dash lines in Fig. 11(b) represent the electric-field lines as expected from electrostatics. In addition to the previous assumptions, we could expect that the displacement distance x of each of the ions is $<< L_D$, or the Debye length. When these conditions are met, the electric field does not decay significantly in the vicinity of the conductive surface, and we assume Eq. (3) to be valid with $E(t)=E_0 \exp(i\omega t)$ keeping x_0 small.

Even though the ODO model is a simplified description of the complex mechanisms involved in the EP effect, there is a clear analogy between the two different approaches described throughout this paper. For example, if we assume a perfectly flat electrode region, for which the double layer behaves as a capacitance, then the potential energy U_C stored in the capacitance has the same functional form as that of a harmonic restoring potential, U_{HO}, as shown below

$$U_C = \frac{1}{2}\frac{Q^2}{C}, \tag{13}$$

$$U_{\mathrm{HO}} = \frac{1}{2}(nAd)kx^2. \tag{14}$$

Here, C and A are the double-layer capacitance and area, respectively, of a flat region of the electrode, and Q is the displacement charge. In addition, n represents the concentration of ions in the double layer, d' is the thickness of a sheet of charge interacting with its image charge in the electrode, and x is the displacement of the sheet of charge from its equilibrium position. When combining Eqs. (13) and (14) using $Q=nqAx$, with q being the charge of each ion, and $C=\epsilon'\epsilon_0 A/d$, we can find a relationship that describes the restoring force constant as follows:

$$k = \frac{nq^2}{\epsilon'\epsilon_0}\frac{d}{d'}. \tag{15}$$

We have considered a linear relationship of displacement charge Q with respect x, which is consistent with the idea that the charge $Q=CV$ increases linearly with the applied voltage as $V=Ex$, particularly in our use of Eq. (3). In this picture, the interaction of the ions and their respective image generated by the rearrangements of charges in the electrode does not follow the electrostatic rule of $1/(2d)^2$ for a single point charge near a conductive plate. Instead, the restoring force generated by the polarization of a sheet of charges generates a linear function with the displacement distance x, as assumed when one is modeling atomic polarizability.

From Figs. 4 and 5 one can expect that the harmonic-oscillator model describes better the data at higher concentrations. This is due to the fact that at these concentrations, we have a double bell-shaped curve in the imaginary part of the conductivity spectrum. This consideration also restricts the validity of the model to concentrations $\sim$10 mM. At concentration $<$10 mM, the real and imaginary parts of the conductivity spectra show an increasing behavior, apparently showing a second resonance at frequencies of $\sim 10^6$. Experi-

mentally, there is a resonance effect that happens with the liquid cell, the connecting lines, and the equipment used for data acquisition. This resonance is dominant for low conductivities, but at higher conductivities the negative values dominate showing the second bell at negative values.

Our experiments are restricted in the frequency range set by the impedance analyzer, and to the artifacts that appear at higher frequencies. Both factors contribute to our inability to verify with good confidence the band pass filter effect that the harmonic oscillator models show. Thus, the goodness of the fit cannot be evaluated as desired. The data obtained from the fit suggest the behavior described by Fig. 11. As already mentioned, we obtain a better fit by eye at low conductivities. However, we know that qualitatively the overdamped oscillator models describe some of the features observe experimentally in Figs. 4 and 5 and when combined for multiple components, the fit is corrected.

Finally, we have to acknowledge the fact that a rough surface might produce nonlinearities in our equation of motion, as well as the decay of the electric potential in the axial direction. However, the data are well described without these nonlinear effects. It is expected that a better agreement with the data could be achieved if such nonlinearities are included in the model.

VI. CONCLUSION

In electrochemistry, one of the main challenges is to understand the interface between an electrode an electrolyte. This effect has been studied widely but no definitive agreement has been reached. Experimentally this effect is minimized by using such methods as varying the spacing between the electrodes, using a four-probe method, or electrodeless techniques [5], but this effect cannot be neglected, especially at low frequencies. Here, we compared two models used to described the electrode polarization effect at lower frequencies. One of the approaches was to consider a polarization impedance given by a CPE into the circuit modeling. This method allows one to fit the data with high accuracy, but when one tries to extract microscopic information about the double layer, it becomes difficult to interpret the results.

Theoretical descriptions of the fractal nature of the roughness of the electrode suggest that the power-law behavior of the CPE could be interpreted as the random walk of ions close to a rough surface described by Halsey-Leibig theory [19]. In addition, we note that the so called "fractal dimension" p changes with the ions used in solution and with concentration, as seen in Fig. 7. The minimal changes in p indicate that the fractal nature not only depends on the surface characteristics of the electrode, but also on the type of solution that is in contact with the electrode. This is supported by the harmonic-oscillator model, where the fitting parameters depend on the properties of the ions in the solution.

Another important parameter while comparing the two models is T, which varies with respect to the electrolyte. This is an indication of the role of the electrolyte in the double layer. T has similar units when compared to σ_m, which could be expressed as Ss/m, when the admittance is multiplied by the geometric factor d/A to obtain units of conductivity instead of admittance, except for the power-law exponent p. Both have different interpretations. When the CPE model is used, T does not change with respect to the concentration, but this is not true for the variation observed with σ_m, which increases as the concentration increases. This is as expected from the definition of σ_m, finding good agreement between theory and experiment. This comparison will be valid only when $p=1$ when the units match.

One of the main discrepancies when one is using the CPE as a model for the fractal properties of the electrode electrolyte interface is that the frequencies should be higher than those observed in this work [19], whereas overdamped oscillatory motion of the ions near the interface gives qualitatively good agreement with the experimental results at the frequencies used here, particularly when the data are fitted with two relaxation processes $i=2$. A better understanding of the differences between divalent and monovalent ions is needed and requires further experimentation.

One suggestion to complete the overdamped oscillator model is to have a fractional harmonic-oscillator model. It has been reported that a fractional harmonic oscillator presents a damping effect similar to the damped oscillator model [25], but the phenomenon comes from the nonlinear operators in fractional derivatives. By combining different components, such as the roughness of the electrode, reaction kinetics close to the interface, and other factors, one can scale the model presented here and give a better physical description of what the double layer is all about.

ACKNOWLEDGMENTS

This work was supported by the State of Texas through the Texas Center for Superconductivity at the University of Houston and by the Robert A. Welch Foundation (E-1221).

[1] H. P. Schwan, *Advances in Biological and Medical Physics* (Academic Press, New York, 1958).
[2] E. H. Grant, R. J. Sheppard, and G. P. South, *Dielectric Behavior of Biological Molecules in Solution* (Oxford University Press, New York, 1978).
[3] Y. Feldman, R. Nigmatullin, E. Polygalov, and J. Texter, Phys. Rev. E **58**, 7561 (1998).
[4] Y. Feldman, E. Polygalov, I. Ermolina, Y. Polevaya, and B. Tsentsiper, Meas. Sci. Technol. **12**, 1355 (2001).
[5] K. Asami, E. Gheorghiu, and T. Yonezawa, Biophys. J. **76**, 3345 (1999).
[6] H. Wakamatsu, Hewlett-Packard J. **48**, 37 (1997).
[7] H. P. Schwan and C. D. Ferris, Rev. Sci. Instrum. **39**, 481 (1968).
[8] R. Tamamushi and K. Takahashi, J. Electroanal. Chem. Interfacial Electrochem. **50**, 277 (1974).

[9] S. Takashima, *Electrical Properties of Biopolymers and Membranes* (Institute of Physics Publishing, Philadelphia, 1989).
[10] C. Prodan, F. Mayo, J. R. Claycomb, and J. H. Miller, Jr., J. Appl. Phys. **95**, 3754 (2004).
[11] C. Prodan, J. R. Claycomb, E. Prodan, and J. H. Miller, Jr., Physica C **341–348**, 2693 (2000).
[12] F. van der Touw and M. Mandel, Trans. Faraday Soc. **67**, 1336 (1971).
[13] F. van der Touw, M. Mandel, D. D. Honijk, and H. G. F. Verhoog, Trans. Faraday Soc. **67**, 1343 (1971).
[14] C. Prodan, Ph.D. thesis, University of Houston, 2003.
[15] H. Sanabria, J. H. Miller, Jr., A. Mershin, R. F. Luduena, A. A. Kolomenski, H. A. Schuessler, and D. V. Nanopoulos, Biophys. J. **90**, 4644 (2006).
[16] I. Wolff, Phys. Rev. **27**, 755 (1926).
[17] B. Sapoval, Annu. Rev. Mater. Sci. **19**, 507 (1989).
[18] F. Bordi, C. Cametti, and R. H. Colby, J. Phys.: Condens. Matter **16**, R1423 (2004).
[19] T. C. Halsey and M. Leibig, Ann. Phys. (N.Y.) **219**, 109 (1992).
[20] T. Pajkossy and L. Nyikos, Phys. Rev. B **42**, 709 (1990).
[21] J. B. Bates, Y. T. Chu, and W. T. Stribling, Phys. Rev. Lett. **60**, 627 (1988).
[22] A. E. Larsen, D. G. Grier, and T. C. Halsey, Phys. Rev. E **52**, R2161 (1995).
[23] J. E. B. Randles, Discuss. Faraday Soc. **1**, 11 (1947).
[24] C. Ho, I. D. Raistrick, and R. A. Huggins, J. Electrochem. Soc. **127**, 343 (1980).
[25] A. A. Stanislavsky, Phys. Rev. E **70**, 051103 (2004).